The Crystal Structure of Bacillus subtilis Lipase

Pouderoyen, Gertie van; Eggert, Thorsten; Jaeger, Karl-Erich; Dijkstra, Bauke W.

Published in:
Journal of Molecular Biology

DOI:
10.1006/jmbi.2001.4659

Publication date:
2001

doi:10.1006/jmbi.2001.4659 available online at http://www.idealibrary.com on IDEAL® J. Mol. Biol. (2001) 309, 215–226

JMB

The Crystal Structure of *Bacillus subtilis* Lipase: A Minimal α/β Hydrolase Fold Enzyme†

Gertie van Pouderoyen[1], Thorsten Eggert[2], Karl-Erich Jaeger[2] and Bauke W. Dijkstra[1]*

[1]*Laboratory of Biophysical Chemistry, University of Groningen, Nijenborgh 4 9747 AG, Groningen, The Netherlands*

[2]*Lehrstuhl für Biologie der Mikroorganismen, Ruhr-Universität Bochum D-44780, Bochum Germany*

**Corresponding author*

The X-ray structure of the lipase LipA from *Bacillus subtilis* has been determined at 1.5 Å resolution. It is the first structure of a member of homology family I.4 of bacterial lipases. The lipase shows a compact minimal α/β hydrolase fold with a six-stranded parallel β-sheet flanked by five α-helices, two on one side of the sheet and three on the other side. The catalytic triad residues, Ser77, Asp133 and His156, and the residues forming the oxyanion hole (backbone amide groups of Ile12 and Met78) are in positions very similar to those of other lipases of known structure. However, no lid domain is present and the active-site nucleophile Ser77 is solvent-exposed. A model of substrate binding is proposed on the basis of a comparison with other lipases with a covalently bound tetrahedral intermediate mimic. It explains the preference of the enzyme for substrates with C_8 fatty acid chains.

Keywords: Bacillus subtilis; lipase; X-ray crystallography; α/β hydrolase fold; esterase

Introduction

Bacillus subtilis is a Gram-positive, aerobic, spore-forming bacterium found in soil and water, and in association with plants. The organism is of substantial commercial interest because of its highly efficient protein secretion system.[1] It is used, for instance, for the production of bulk quantities of proteases and amylases.[2]

B. subtilis produces and excretes lipases, which catalyse both the hydrolysis and the synthesis of long-chain triacylglycerols. Because of their wide diversity in substrate specificity, lipases have found important industrial applications in the resolution of racemic mixtures, the synthesis of esters and in transesterification reactions. Moreover, they are used as an additive in laundry detergents.[3,4]

Extracellular lipolytic activity of *B. subtilis* was first observed in 1979.[5] Molecular research started in 1992 when a lipase gene, *lipA*, was cloned, sequenced and overexpressed, and the protein was characterised.[6–8] Later, a second gene, *lipB*, which is 68 % identical with *lipA* at the nucleic acid level, was found as a result of the *B. subtilis* genome-sequencing project.[9] This gene has been cloned and overexpressed as well, the protein was purified, and its substrate specificity has been determined.[10]

The *B. subtilis* lipase LipA is particularly interesting, since its molecular mass (19,348 Da, 181 amino acid residues) is much smaller than that of the lipases from other organisms. Furthermore, this enzyme represents one of the few examples of a lipase that does not show interfacial activation in the presence of oil-water interfaces.[6] Moreover, LipA is very tolerant to basic pH and has even its optimum activity at pH 10.0. It was classified as a lipase rather than an esterase, because it is able to hydrolyse *sn*-1 and *sn*-3 glycerol esters with long fatty acid chains.[7] Nevertheless, its highest activity is on glycerol esters with medium-length (C_8) fatty acid chains, thus resembling an esterase in this respect.[7,10]

Several structures of larger lipases have been elucidated.[4] They all have an α/β hydrolase fold,[11–13] with most of them containing a helical segment called the lid that covers the active site when the enzyme is in the so-called closed conformation. In the presence of lipid aggregates, the lid opens, and the enzyme activity is increased, a phenomenon called interfacial activation.[13] The absence of such an interfacial activation of *B. subtilis* lipase, together with its small size, suggests that

†This paper is dedicated to the memory of Professor Charles Colson, Louvain-la-Neuve, who initiated the molecular research on *Bacillus subtilis* lipase.

E-mail address of the corresponding author: bauke@chem.rug.nl

0022-2836/01/010215–12 $35.00/0

it does not have a lid. Two other small α/β hydrolase fold enzymes without lids are known. They are cutinase from *Fusarium solani*[14,15] and acetylxylan esterase from *Penicillium purpurogenum*.[16] These enzymes have an accessible active site, with an intact preformed oxyanion hole, which stabilises the negatively charged reaction intermediates. However, their sequences do not show any homology to the *B. subtilis* lipase sequence, and thus it remained an open question whether the *B. subtilis* lipase active site resembles those of cutinase and acetylxylan esterase.

Bacterial lipases are currently classified into eight families,[17] with true lipases forming family I, the largest family, which contains six subfamilies. *Bacillus* lipases have been placed in subfamilies 4 and 5. These two subfamilies have in common that alanine replaces the first glycine residue in the conserved G-X-S-X-G pentapeptide around the active-site serine residue. Subfamily 4 consists of only three members, LipA and LipB from *B. subtilis*, and a lipase from *Bacillus pumilis*, which share 74-77 % sequence identity. With a mass of 19 kDa they are the smallest true lipases known and share very little sequence similarity (about 15 %) with the other, much larger, *Bacillus* lipases that constitute subfamily 5. Here, the first 3D structure of a member of family I.4 is described.

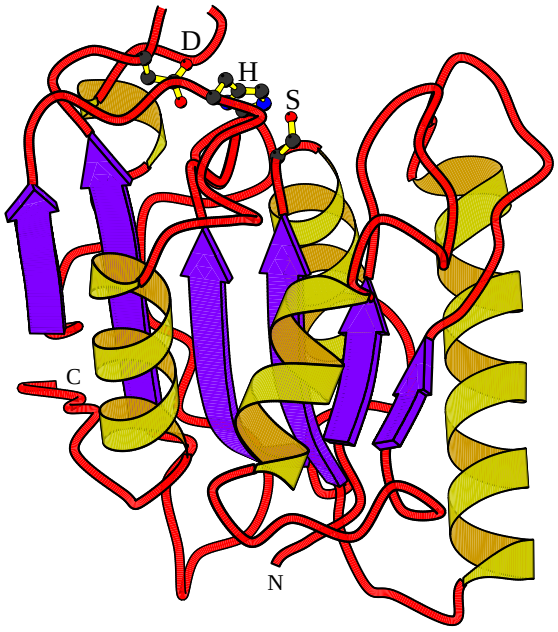

Figure 1. A representation of the structure of *B. subtilis* lipase. The catalytic triad residues, Ser77, His156 and Asp133, are labelled with S, H and D, respectively. The letters N and C indicate the N and C termini, respectively.

Results and Discussion

General features of the structure

The *B. subtilis* lipase has a globular shape with dimensions of 35 Å × 36 Å × 42 Å (see Figure 1). The structure shows a single compact domain that consists of six β-strands in a parallel β-sheet, surrounded by α-helices. There are two α-helices on one side of the β-sheet and three on the other side (including a very small one of only four amino acid residues).

The fold of *B. subtilis* lipase resembles that of the core of the α/β hydrolase fold enzymes,[11] as do the other lipases of which the 3D structure has been elucidated. A comparison of the secondary structure elements of *B. subtilis* lipase and the canonical α/β hydrolase fold (Figure 2(a) and (b)) shows that *B. subtilis* lipase lacks the first two β-strands (β1 and β2) of the canonical fold and that helix αD is replaced by a small 3_{10} helix. Furthermore, helix αE is exceptionally small, with only one helical turn, and several α-helices start or terminate with 3_{10} helical turns (according to the program DSSP,[18] see Figure 2(b)). There is no separate lid domain present, as for instance in the larger lipases.[13] Because of its small size and the absence of a lid domain, *B. subtilis* lipase can thus be considered as a minimal α/β hydrolase fold enzyme.

Two molecules in the asymmetric unit

There are two lipase molecules in the asymmetric unit of the $P2_12_12_1$ space group, called A and B. They are related by a rotation of 169° about an axis in a general orientation. The N termini of both molecules approach each other, but the electron density for the first N-terminal residues is not unambiguously interpretable. Ala1 is not well defined in both molecules, nor is Glu2 in molecule A. In contrast, Glu2 of molecule B is clearly visible in density, with its side-chain hydrogen bonded to Lys170 and Asn174 of molecule A. Although the electron density for the N-terminal residues (Ala1 and Glu2 of molecule A, and Ala1 of molecule B) is blurred, it clearly extends towards a spherical density. Since this latter density has a significant level (>5σ), is spherical, is between the two molecules of the asymmetric unit, and since Cd^{2+} (or Zn^{2+}) is essential for crystallization, it seems likely that Cd^{2+} is bound to the N termini. Therefore, we included a cadmium ion in the final model. However, the precise interactions of the N termini with the ion remain elusive. The *B*-factor of this Cd^{2+} is about 40 Å^2, while the *B*-factors of the nearest amino acid residues (His3 of molecule A and Glu2 of molecule B) are about 25 Å^2. The higher *B*-factor of the Cd^{2+} could indicate that the Cd^{2+} position is not fully occupied in the crystal. This might explain the blurred density for the N-terminal residues that are only partly bound and ordered when Cd^{2+} is present. Since gel filtration and dynamic light-scattering studies give no indications of oligomerisation (see Materials and Methods), molecules

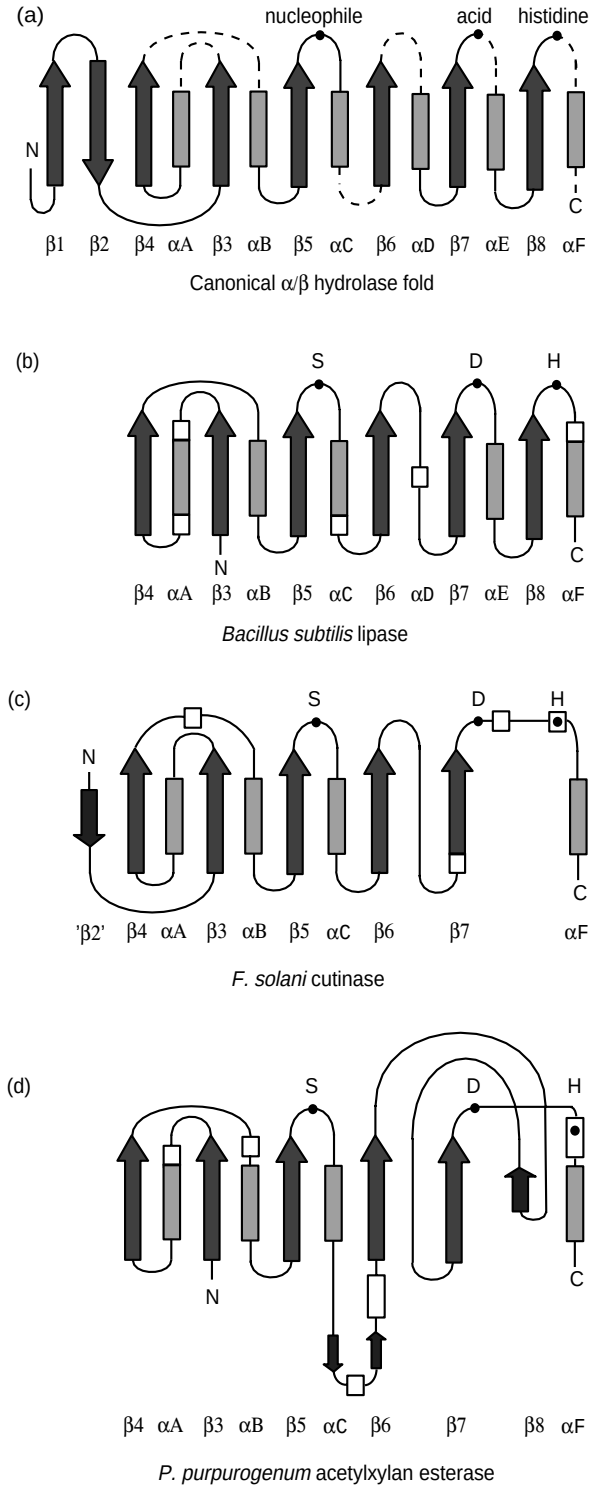

Figure 2. Secondary structure topology of (a) the canonical α/β hydrolase fold, (b) *B. subtilis* lipase, (c) *F. solani* cutinase and (d) *P. purpurogenum* acetylxylan esterase. The broken lines in (a) indicate loops of variable length.

A and B are unlikely to represent a functional dimer.

The r.m.s. difference in C^{α} positions of molecules A and B is 0.85 Å (residues 3 to 181). The largest differences occur in two neighbouring loops, Ile12-Ser16 and Lys44-Thr45. In molecule A, these loops are freely accessible from a solvent channel, while in molecule B they are involved in crystal contacts. This suggests that molecule A most likely represents the most abundant conformation in solution and that the conformations of the loops in molecule B are probably affected by the crystal packing.

When these loops are left out of the comparison, the r.m.s. difference in C^{α} positions of the remaining 172 amino acid residues is reduced to 0.46 Å. However, Luzzati and SigmaA plots[19,20] indicate that the statistically expected r.m.s. difference would be between 0.15 and 0.20 Å. The largest variations in C^{α} positions occur in the α-helices and loops, but not in the central β-sheet. This indicates that the residues away from the core β-sheet have some conformational freedom.

The catalytic triad

In lipases, the active-site residues are Ser, Asp/Glu and His.[11] They always occur in this order in the amino acid sequence, with Ser being the nucleophile. On the basis of a multiple sequence alignment of several microbial lipases, Ser77 was suggested to be the nucleophile in *B. subtilis* lipase[6] and Asp133 was proposed as the catalytic acid.[21] The S77C and D133N mutants were indeed devoid of lipase activity.[22] For the active-site histidine residue, two candidates were present initially, His152 and His156. As an H152N mutant showed activity comparable to that of wild-type lipase A, it was concluded that His156 is most likely the catalytic histidine residue.[22,23]

These assignments are in agreement with our 3D structure. Ser77, Asp133 and His156 are arranged in a catalytic triad-like configuration. Ser77 is positioned at a very sharp turn between strand β5 and helix αC, the so-called nucleophile elbow. Its main chain ϕ,ψ angles are outside the favoured regions of the Ramachandran plot (52°, −127° and 51°, −122° for molecules A and B, respectively), as is common for the nucleophile in α/β hydrolase fold enzymes,[13] Asp133 is located at the end of strand β7, and His156 is situated in the loop following strand β8. These locations and the relative orientations of the side-chains are similar to those found in other lipases.

Ala75, which occurs instead of the first Gly in the G-X-S-X-G consensus sequence around the active-site Ser77, has a conformation very similar to that of the Gly residues in other lipases. Its ϕ,ψ angles are −126°, 140° and −118°, 143° for molecules A and B, respectively. They are typical ϕ,ψ angles for a β-strand conformation. An alanine instead of a glycine residue does therefore not

greatly affect the main-chain conformation of the nucleophile elbow.

Comparison with other α/β hydrolases

From a DALI structure alignment, it appears that *B. subtilis* lipase is most similar in structure to the core of the much larger lipase B from the yeast *Candida antarctica*.[24] The r.m.s. difference of the 163 aligned C^{α} atoms is 1.9 Å. It could be considered remarkable that *B. subtilis* lipase resembles more closely a fungal lipase than other bacterial lipases, although these organisms are phylogenetically quite distinct. One possible explanation could be that, similar to *B. subtilis* LipA, the *C. antarctica* lipase B has the first glycine residue in the Gly-X-Ser-X-Gly lipase consensus motif replaced. The threonine residue in *C. antarctica* lipase B at this position and the alanine residue in *B. subtilis* LipA restrict the close approach of strand β5 and helix αC, the secondary structure elements flanking the nucleophile elbow.[24] Compared to other lipases, helix αC in these two enzymes is more bent away from strand β5, thus rationalising the structural agreement between the *B. subtilis* and *C. antarctica* lipases.

So far, the 3D structures of two other small (~20 kDa) α/β hydrolase fold enzymes without lid have been elucidated, cutinase and acetylxylan esterase. Figures 3 and 4 show a DALI structural comparison[25] of *B. subtilis* lipase with these enzymes. Although the structures appear similar, the C^{α} atoms of *B. subtilis* lipase superimpose with a rather high r.m.s. difference of 2.8 Å (145 out of 197 C^{α} atoms for cutinase), and 2.9 Å (148 out of 207 for acetylxylan esterase), respectively. Nevertheless, five β-strands (β3 to β7) are common in the three structures as well as four α-helices (αA, αB, αC and αF).

B. subtilis is the smallest (181 amino acid residues) of these three enzymes. The additional amino acid residues of cutinase (197 amino acid residues) form an N-terminal extension at the position of the canonical α/β hydrolase fold strand β2 (Figure 2(c)) and the loops are generally longer, also in the lid region. On the other hand, cutinase lacks the canonical αE and β8 secondary structure elements, which are present in *B. subtilis* lipase (Figures 2(b) and (c), and 3).

Acetylxylan esterase has 207 amino acid residues. The additional residues are located in longer loop regions, between strand β4 and helix αB, and between helix αC and strand β6. The C-terminal region of acetylxylan esterase is folded differently, with a β-strand at position β8 inserted between strands β6 and β7 (Figures 2(b) and (d), and 4).

The active-site cleft

Because no lid is present, the active site of *B. subtilis* lipase is solvent-exposed. It is located at the bottom of a small cleft between two loops consisting of residues 10 to 15 and 131 to 137. Compared to the active sites of cutinase and acetylxylan esterase, the cleft is shallower and wider, because the loops lining the cleft are shorter and do not extend as much from the core of the protein (Figures 3 and 4).

To obtain insight into substrate binding, substrate preference and enantioselectivity of *B. subtilis* lipase, we compared its structure with those of lipases with a covalently bound inhibitor in the active site. There are three structures known of lipases with a covalently bound triglyceride analogue.[26–28] These inhibitors (Figure 5(a) and (b)) bind covalently with their phosphonyl group to the active-site serine residue, mimicking the first tetrahedral intermediate in the cleavage reaction of the natural triacylglycerol substrates (Figure 5(c)). The binding mode of these inhibitors in the various lipases is remarkably similar. One of the phosphonyl oxygen atoms is bound in the so-called oxyanion hole by two peptide NH groups. The catalytic histidine N^{ε} is at hydrogen bonding distance from the active-site serine O^{γ} and the ester oxygen atom between the phosphorus atom and the glycerol backbone (Figure 5(d)). The *sn*-3 moiety of the inhibitor points in the same direction in all three lipases, away from the glycerol backbone. In contrast, further away from the phosphonyl group, the positions and directions of the *sn*-1, *sn*-2 and *sn*-3 chains vary.

A superposition of the active sites of *B. subtilis* lipase and the lipases with a covalently bound substrate analogue shows that the *B. subtilis* lipase active-site residues (Ser77, Asp133 and His156) are in very similar positions and orientations compared to those in the inhibitor bound lipases. This is true also for the oxyanion hole, which is formed by the backbone nitrogen atoms of the residue immediately following the nucleophile and a residue located between strand β3 and helix αA.[13] Although in *B. subtilis* lipase no substrate analogue is bound, the oxyanion hole seems to be present intact at the conserved position. It is formed by the peptide NH atoms of Met78 and Ile12. This shows that *B. subtilis* lipase has a pre-formed oxyanion hole like cutinase,[26] but in contrast to e.g. the lipase from *Burkholderia cepacia* (formerly named *Pseudomonas cepacia*), which needs a conformational change upon lid opening to form the oxyanion hole.[29]

In the three inhibited lipases, the phosphonyl group of the tetrahedral intermediate mimic is bound in a very similar way and orientation (Figure 5(d)). Assuming that this will also be the case for *B. subtilis* lipase, we made a model of *B. subtilis* lipase with a covalently bound inhibitor. We retained the position and interactions of the phosphonyl group. The directions of the *sn*-1, *sn*-2 and *sn*-3 chains away from the phosphonyl group were optimised manually to fit in the hydrophobic grooves on the surface of the *B. subtilis* lipase molecule.

Figure 3. Stereo view of the C^{α} traces of the *B. subtilis* lipase in black (top) and *F. solani* cutinase in grey (bottom). The C termini (C), N termini (N) and active sites (AS) are indicated. A superposition of *B. subtilis* lipase and *F. solani* cutinase is given in the middle.[40]

The result is shown in Figure 6. The hydrophobic residues Leu108, Leu140, Ala105, Met78, Ile135 and Ile12 are close to the *sn*-3 chain in this model. Ile157, Leu160, Tyr161, Asn18, Ala15, Phe17, Ile135, Gly155 and Met134 are residues that are likely to play a role in *sn*-1 and *sn*-2 binding. As can be seen from Figure 6, the *B. subtilis* lipase surface easily accommodates lipid molecules with fatty acid chains of up to eight carbon atoms. Longer chains would probably stick out of the pro-

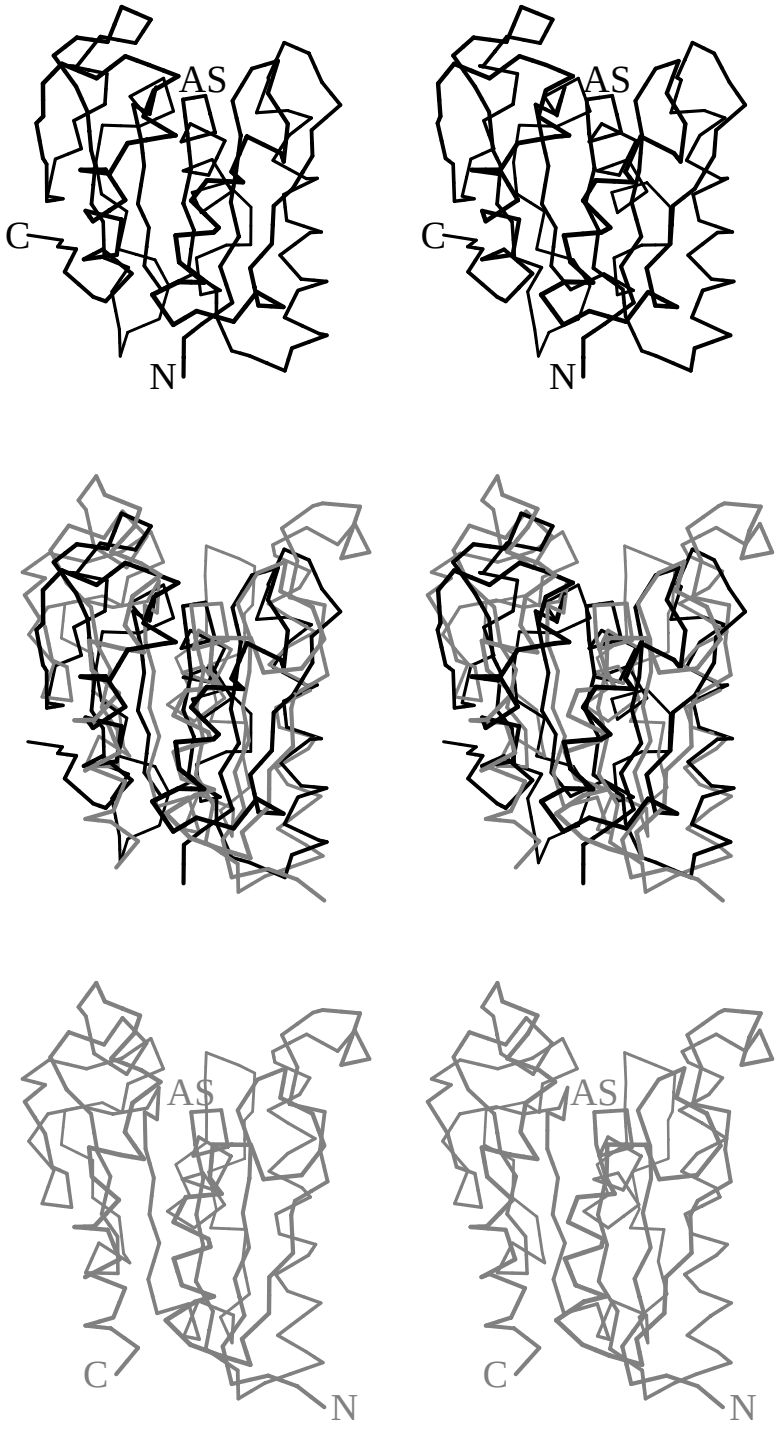

Figure 4. Stereo view of the C^{α} traces of the *B. subtilis* lipase in black (top) and *P. purpurogenum* acetylxylan esterase in grey (bottom). The C termini (C), N termini (N) and active sites (AS) are indicated. A superposition of *B. subtilis* lipase and *P. purpurogenum* acetylxylan esterase is given in the middle.[40]

tein surface into the solvent and would not be stabilised by hydrophobic residues on the surface of the molecule. In this way, it can be rationalised that the *B. subtilis* lipase has its highest activity on triacylglycerol molecules with C_8-chains.[7,10]

Stereospecificity

B. subtilis lipase shows a very small difference in reactivity towards *C*2-glycerol backbone stereoisomers.[10] In *B. cepacia* lipase with a bound inhibitor, the experimentally determined stereospecificity

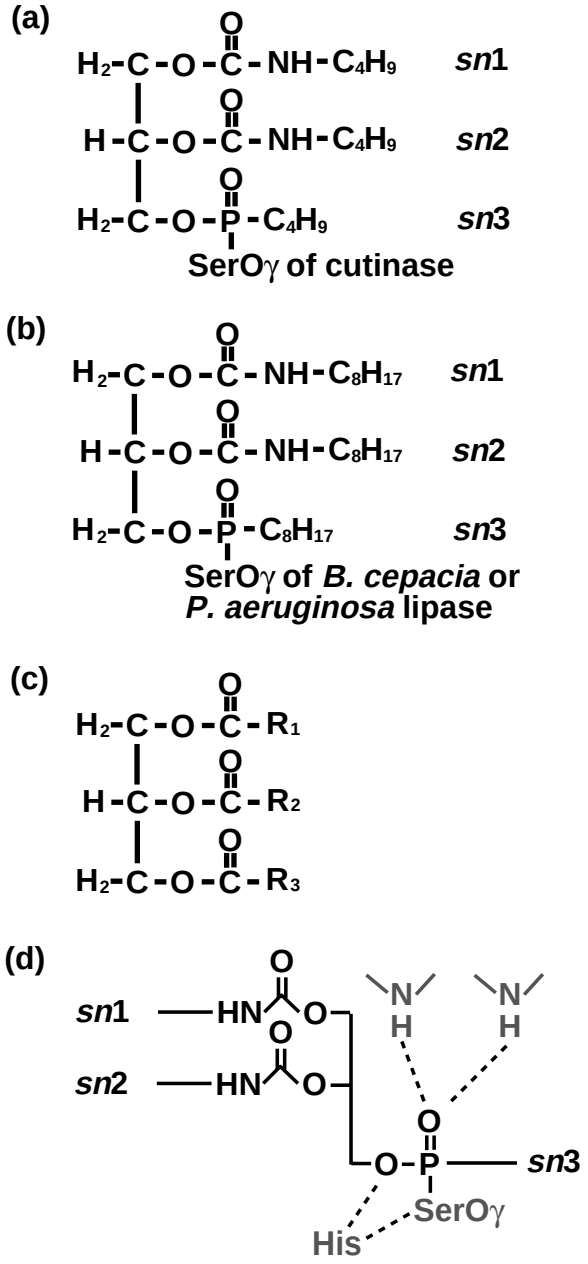

Figure 5. A representation of the phosphonate inhibitors bound to (a) *F. solani* cutinase,[26] (b) *B. cepacia*[27] and *P. aeruginosa* lipase,[28] in comparison with the natural substrate (c) triacylglycerol. (d) A representation of the hydrogen-bonding network around the phosphonyl group.

around the C-2 glycerol backbone atom could be explained by a specific hydrogen bonding interaction of Thr18 with the carbonyl oxygen atom of the *sn*-2 chain.[27] In agreement with the low stereoselectivity of *B. subtilis* lipase, there is no such hydrophilic amino acid residue present at a position equivalent to Thr18 in *B. cepacia* lipase. Instead, Asn18 of *B. subtilis* lipase (which occupies a position different from Thr18 in *B. cepacia* lipase) is at interacting distance from the scissile bond carbonyl oxygen atom of both substrate enantiomers. This residue might therefore contribute to the stereoselectivity of *B. subtilis* lipase. However, the observed stereoselectivity of *B. subtilis* lipase towards natural triacylglycerols is very low, and the contribution of Asn18 to the stereoselectivity must be minor. Nevertheless, Asn18 might contribute to the stereoselectivity on other substrates. Recently, it was observed that *B. subtilis* LipA hydrolysed benzyl, naphthyl and menthyl esters with high enantioselectivity, albeit at a low reaction rate (M.T Reetz *et al.*, unpublished results). Since these substrates are industrially important, the *B. subtilis* lipase may prove to be a valuable biocatalyst for biotechnological applications.

Comparison of lipases A and B from *B. subtilis*

The second *B. subtilis* lipase, LipB, consists of 182 amino acid residues, and is 74 % identical with LipA (see Figure 7 for the sequence alignment). The one additional amino acid residue precedes Ala1 of LipA.[10] The 45 residues that are different are generally located on the surface of the molecule and not clustered at a particular spot. Two substitutions are located in the core of the protein: Val96 of LipA into Ile97 in LipB, and Met8 of LipA into Leu9 in LipB. These two residues are >10 Å apart, and the small differences in size of their side-chains can probably be accommodated by slight adjustments of nearby residues. A view of the active-site cleft (Figure 8) shows that the amino acid differences between LipA and LipB are not close to the active site, but occur mainly at the edge of the active-site surface region. Gly13 of LipA (Ser14 in LipB) and Met134 of LipA (Gln135 in LipB) are closest to the active-site serine residue at a distance of about 9 Å.

Like LipA, LipB has the highest specific activity on C_8 triacylglycerol substrates, but its activity is about 40 % higher than that of LipA. LipB, however, is unable to hydrolyse long (C_{18}) triacylglycerol substrates, which LipA can hydrolyse.[10] Since LipA and LipB have the same size, and since the hydrophobic surfaces around the active site are very similar, this can explain the preference for C_8 substrates of both LipA and LipB, but the inability of LipB to hydrolyse long triacylglycerol substrates is more difficult to explain. As a hypothesis, we suggest that the variation in amino acids at the rim of the active-site surface could contribute to the different behaviour of LipA and LipB towards long (C_{18}) substrates. These differences in amino acids could have an effect on both the binding of single substrate molecules in the active site or on the interaction of the enzyme with substrate-water interfaces.

Conclusions

The crystal structure of *B. subtilis* lipase A is the first 3D structure of a member of homology family

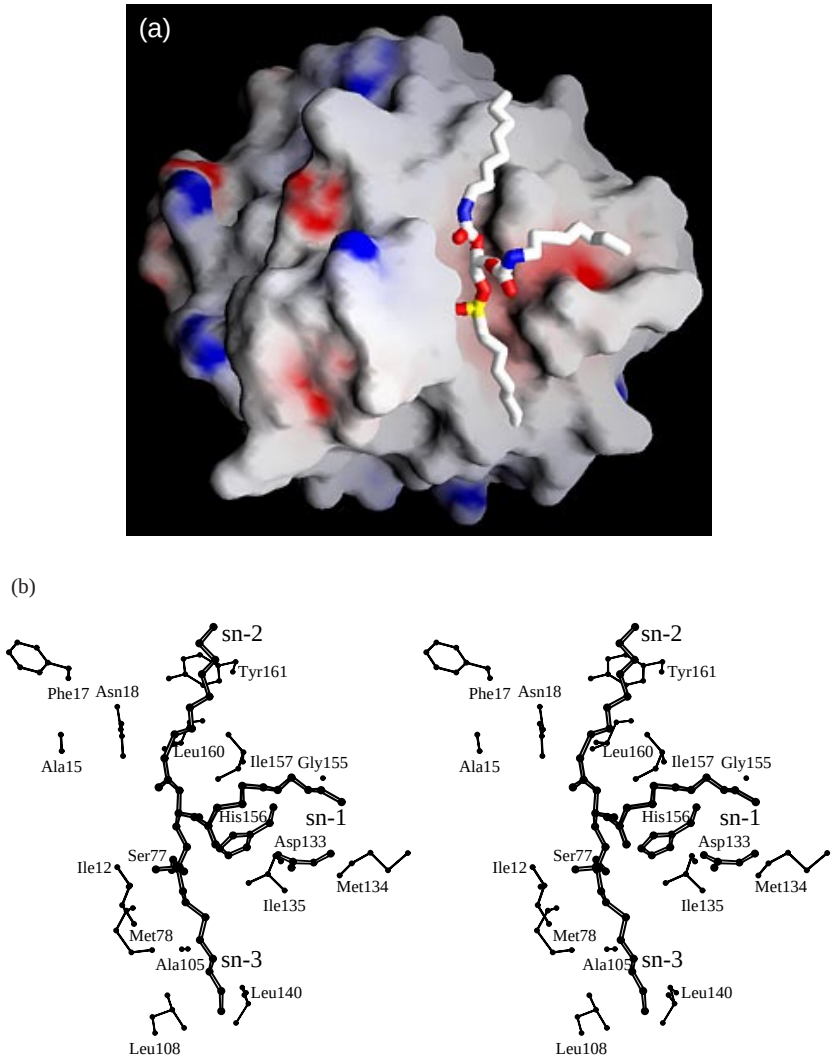

Figure 6. View of a model of the C_8 inhibitor in the active site of *B. subtilis* lipase. (a) The protein is shown in an electrostatic surface representation with positively and negatively charged regions in blue and red, respectively (GRASP scale −30 to +30). The modelled inhibitor is shown in stick representation, with carbon in white, nitrogen in blue, oxygen in red and phosphorus in yellow. (b) Stereo view.[40]

I.4 of bacterial lipases. The molecule has a compact globular shape and has no lid domain. It can be considered as a minimal α/β hydrolase fold enzyme. The active-site residues, Ser77, Asp133 and His156, and the backbone amide groups of residues Ile12 and Met78 forming the oxyanion hole are in positions very similar to those of other known lipase structures. From a comparison with other lipases, which have a covalently bound substrate mimic in the active site, we suggest that the C_8 acyl chains of a substrate are bound on the protein surface, and stabilised by hydrophobic interactions with protein residues. Since the terminal methyl groups of the C_8 chains reach the rim of the hydrophobic surface, it can be rationalised that trioctylglycerol is the preferred substrate of *B. subtilis* lipase. The known 3D-structure of this lipase, and the fact that it can easily be overexpressed and purified from *E. coli*, make this enzyme a very interesting candidate for optimisation by directed evolution.

Materials and Methods

Optimisation of purification

The gene of *B. subtilis* lipase (*lipA*) has been cloned,[6] and the protein has been overexpressed, purified[7] and crystallized.[22,30]

To obtain better yields (30 mg of pure protein from one litre of culture), the production and purification procedure was adapted as follows. *B. subtilis* BCL1051 was grown aerobically for seven hours at 37 °C in three 5-l Erlenmeyer flasks, each containing 0.5 l of medium as described,[7] but with 0.1 M instead of 1 M KH_2PO_4/K_2HPO_4 buffer (pH 7.0). The culture medium was inoculated at 2 % (v/v) with 10 ml pre-cultures. After growth and centrifugation of the cells, the culture supernatant was loaded directly onto a hydrophobic interaction col-

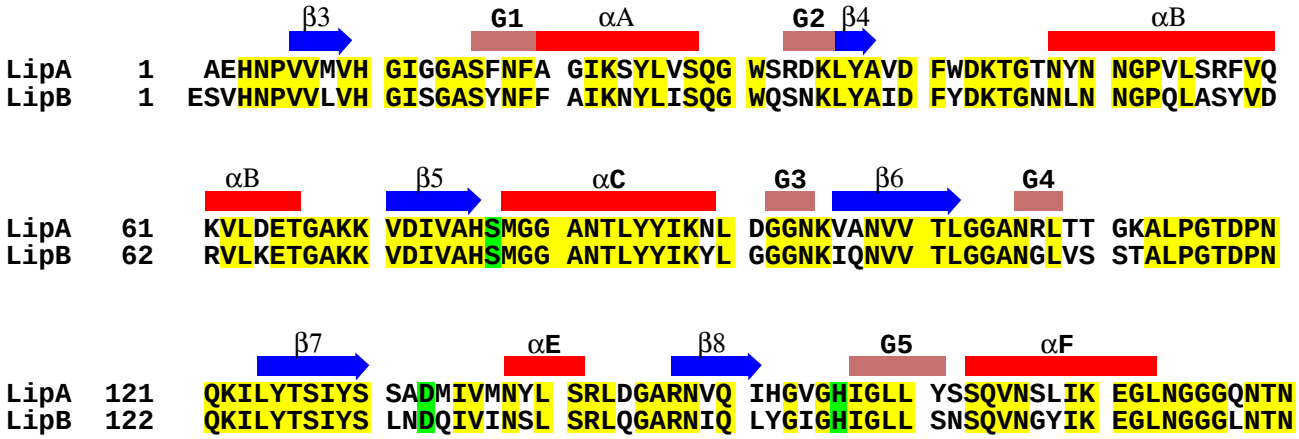

Figure 7. Sequence alignment of LipA and LipB. Identical residues are boxed in yellow and the catalytic triad residues are highlighted in green. Secondary structure elements occurring in LipA are indicated. G1 to G5 are 3_{10} helices.

umn (30 ml Phenyl Sepharose 6 FF (low sub), Pharmacia) pre-equilibrated with 0.1 M potassium phosphate (pH 8.0), at 5 °C. After washing with 10 mM potassium phosphate buffer (pH 8.0), and with 30 % (v/v) ethylene glycol in 10 mM potassium phosphate buffer (pH 8.0), the lipase was eluted with 50 % ethylene glycol in 10 mM potassium phosphate buffer (pH 8.0). Fractions containing lipase activity against *p*-nitrophenylpalmitate[7] were pooled (85 ml). The pooled fractions were diluted 1:1 (v/v) with 50 mM bicine buffer (pH 8.5), prior to loading onto a cation-exchange column (Hitrap SP, Pharmacia) at 9 °C. Maximally, 40 ml was loaded onto a 5 ml column. The column was washed with 50 mM bicine buffer (pH 8.5), and the lipase was eluted with a linear gradient from 0 to 300 mM NaCl in 50 mM bicine buffer (pH 8.5). The fractions containing the lipase were pooled and dialysed overnight against 2 mM glycine buffer (pH 10.0), at 5 °C and concentrated to approximately 6 mg ml^{-1} in a Macrosep (10 K) centrifugal concentrator (Filtron) for use in crystallization experiments. The lipase was stored at −20 °C. The lipase was pure, as judged from a silver-stained SDS-PAGE gel (data not shown).

Determination of the N-terminal sequence of the purified lipase revealed the predicted amino acid sequence. To check whether the pure lipase was not aggregated, an analytical gel-filtration column (Superdex 200 HR 10/30, Pharmacia) was run with 20 mM glycine, 150 mM NaCl (pH 10.0). The lipase eluted as one sharp peak at a volume that corresponded to an apparent molecular mass that is smaller (<10 kDa) than expected (19 kDa), but with no aggregates in the void volume. In addition, dynamic light-scattering measurements were carried out with a solution of 6 mg/ml protein in 2 to 6 mM glycine buffer (pH 10). These experiments showed only monomeric protein. It is therefore unlikely that LipA forms multimers in solution at pH 10.

Crystallization and data collection

Previous crystallization conditions yielded crystals in space group *C*2, which diffracted to 2 Å resolution.[22,30] A better-diffracting crystal form (space group $P2_12_12_1$) was obtained by omitting the *n*-octyl-β-D-glucoside, but adding 3 mM $CdCl_2$ or 10 mM $ZnCl_2$ to the reservoir (containing 35 % PEG4000, 0.1 M ethanol amine (pH 10.0), and 20 mM Na_2SO_4). Drops were made by mixing 3 µl of lipase solution with 3 µl of reservoir. This new crystal form diffracts to 1.5 Å resolution using synchrotron radiation (see Table 1, native) when flash-frozen in liquid nitrogen directly from the drop in which it was grown.

All data were processed and scaled using the programs DENZO and SCALEPACK.[31] Reduction to structure factor amplitudes was performed with TRUNCATE.[32]

Table 1. Data collection

Soak	Native	K_2PtCl_4	$HgCl_2$
Source	ESRF, ID14-4	DESY, BW7B	DESY, BW7B
Resolution measured (Å)	1.5	2.0	2.5
Resolution used (Å)		2.5	2.5
Space group	$P2_12_12_1$	$P2_12_12_1$	$P2_12_12_1$
a (Å), *b* (Å), *c* (Å)	39.64, 83.20, 95.75	39.15, 82.37, 94.95	39.52, 82.75, 94.92
β (deg.)	90	90	90
Molecules/asymmetric unit	2	2	2
Reflections	689,356	180,931	113,335
Unique reflections	41,851	20,948	11,131
Completeness (%)	82.4 (30.6)	97.2 (60.6)	98.0 (90.6)
R_{merge} (%)	7.6 (28.0)	5.0 (9.9)	12.6 (14.8)

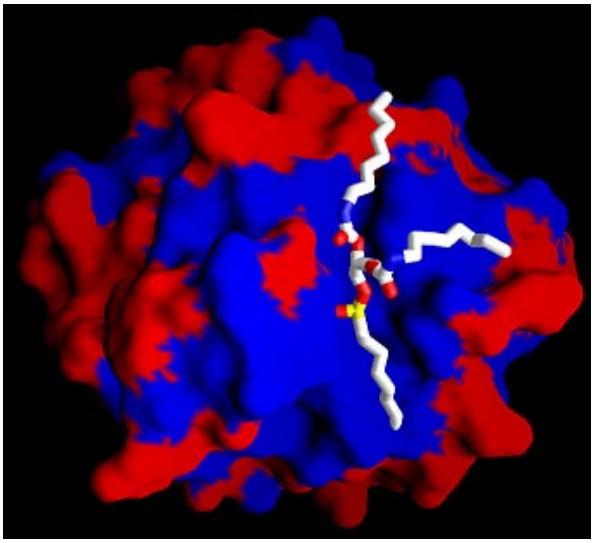

Figure 8. View of the surface of LipA around the active site with the modelled C_8 substrate. Amino acid residues that are identical in LipA and LipB are coloured blue and those that are different in LipB are indicated in red.

Heavy-atom derivatives, phasing and density modification

Heavy-atom derivatives were prepared by soaking crystals grown in the presence of Cd^{2+} overnight in 42 % PEG4000, 0.1 M ethanol amine (pH 10.0), 20 mM Na_2SO_4, 5 mM K_2PtCl_4 or 5 mM $HgCl_2$, and flash-frozen in liquid nitrogen. Data were collected at the EMBL outstation at DESY, Hamburg (Table 1). The anomalous Patterson map of the Pt derivative showed one consistent very clear peak in each of the three Harker sections. It was obvious that this was a derivative. A cross-Fourier of the initial Pt phases with the Hg derivative data gave two potential Hg sites. With the program SHARP[33] and the MIRAS method, the heavy-atom positions were refined. Additional heavy-atom sites present in the residual maps were added (see Table 2). The overall figure of merit for the acentric reflections was 0.54 using all data to 2.5 Å resolution. Solvent flattening with 38 % solvent was done with DM.[34] In the resulting electron density map, a β-sheet and several α-helices were recognisable.

Table 2. Phasing statistics

	K_2PtCl_4	$HgCl_2$
Sites	5	12
R_{cullis} (acentric) iso/ano	0.90/0.73	0.83/0.83
Phasing power (iso) centric/acentric	0.93/1.08	1.26/1.54
Phasing power (ano) acentric	1.87	1.30
Overall Figure of merit (acentric)	0.54	
Overall Figure of merit (centric)	0.45	

Model building, refinement and analysis

With the program wARP,[35,36] the phases were improved and extended to 1.5 Å resolution. The model was auto traced,[37] including most of the side-chains. Of the 362 amino acid residues (two molecules of 181 amino acid residues each in the asymmetric unit), 344 were positioned correctly. After changing a few side-chains and adding a few amino acid residues, the model was refined with CNS[38] until the structure did not converge further. The *R*-factor is 18.1 % (1.5 Å native) and R_{free} is 20.6 %. After a final refinement step including the R_{free} set, the *R*-factor became 17.7 %. The final model contains residues 3-181 of molecule A and residues 2-181 of molecule B, 518 water molecules and one Cd^{2+} in the asymmetric unit. Residues Ala1 and Glu2 (of molecule A), and Ala1 and residues 13 to 17 (of molecule B) are not clear in density, but the rest of the model is fully covered by electron density.

The geometry of the final model was analysed using PROCHECK:[39] 90 % of the residues are in the most favoured regions of the Ramachandran plot and no residues are in disallowed regions. The r.m.s. deviation from ideality in bond length is 0.005 Å and in bond angles 1.2°.

Protein Data Bank accession code

The co-ordinates have been deposited with the RCSB Protein Data Bank with accession code 1I6W.

Acknowledgements

This work was supported by the European Commission in the framework of the Biotechnology programme (project no. BIO4-CT98-0249). S. Ransac, K. Schanck and M. Blaauw are thanked for their earlier contributions to this project. All members of the Protein Crystallography Group are thanked for data collection and useful discussions. We thank the staff of the protein crystallography beam lines at EMBL-DESY, Hamburg, at the ESRF, Grenoble, and at the MAX-Lab, Lund, for the synchrotron data collection facilities and assistance. The collaborators in the EU project, Dr Bertus van den Burg, Bart van Montfort, and Luca Jovine are thanked for stimulating discussions.

References

1. Tjalsma, H., Bolhuis, A., Jongbloed, J. D., Bron, S. & van Dijl, J. M. (2000). Signal peptide-dependent protein transport in *Bacillus subtilis*: a genome-based survey of the secretome. *Microbiol. Mol. Biol. Rev.* **64**, 515-547.
2. Harwood, C. R. (1992). *Bacillus subtilis* and its relatives: molecular biological and industrial workhorses. *Trends Biotechnol.* **10**, 247-256.
3. Jaeger, K. E. & Reetz, M. T. (1998). Microbial lipases form versatile tools for biotechnology. *Trends Biotechnol.* **16**, 396-403.
4. Jaeger, K.-E., Dijkstra, B. W. & Reetz, M. T. (1999). Bacterial biocatalysts: molecular biology, three-dimensional structures, and biotechnological applications of lipases. *Annu. Rev. Microbiol.* **53**, 315-351.
5. Kennedy, M. B. & Lennarz, W. J. (1979). Characterization of the extracellular lipase of *Bacillus subtilis*

and its relationship to a membrane-bound lipase found in a mutant strain. *J. Biol. Chem.* **254**, 1080-1089.
6. Dartois, V., Baulard, A., Schanck, K. & Colson, C. (1992). Cloning, nucleotide sequence and expression in *Escherichia coli* of a lipase gene from *Bacillus subtilis* 168. *Biochim. Biophys. Acta,* **1131**, 253-260.
7. Lesuisse, E., Schanck, K. & Colson, C. (1993). Purification and preliminary characterization of the extracellular lipase of *Bacillus subtilis* 168, an extremely basic pH-tolerant enzyme. *Eur. J. Biochem.* **216**, 155-160.
8. Dartois, V., Coppee, J. Y., Colson, C. & Baulard, A. (1994). Genetic analysis and overexpression of lipolytic activity in *Bacillus subtilis*. *Appl. Environ. Microbiol.* **60**, 1670-1673.
9. Kunst, F., Ogasawara, N., Moszer, I., Albertini, A. M., Alloni, G., Azevedo, V., Bertero, M. G., Bessières, P., Bolotin, A., Borchert, S., Borriss, R., Boursier, L., Brans, A., Braun, M. & Brignell, S. C. *et al*. (1997). The complete genome sequence of the Gram-positive bacterium *Bacillus subtilis*. *Nature,* **390**, 249-256.
10. Eggert, T., Pencreac'h, G., Douchet, I., Verger, R. & Jaeger, K.-E. (2000). A novel extracellular esterase from *Bacillus subtilis* and its conversion to a monoacylglycerol hydrolase. *Eur. J. Biochem.* **267**, 6459-6469.
11. Ollis, D. L., Cheah, E., Cygler, M., Dijkstra, B., Frolow, F., Franken, S. M., Harel, M., Remington, S. J., Silman, I., Schrag, J., Sussman, J. L., Verschueren, K. H. G. & Goldman, A. (1992). The α/β hydrolase fold. *Protein Eng.* **5**, 197-211.
12. Schrag, J. D. & Cygler, M. (1997). Lipases and α/β hydrolase fold. *Methods Enzymol.* **284**, 85-107.
13. Nardini, M. & Dijkstra, B. W. (1999). α/β Hydrolase fold enzymes: the family keeps growing. *Curr. Opin. Struct. Biol.* **9**, 732-737.
14. Martinez, C., de Geus, P., Lauwereys, M., Matthyssens, M. & Cambillau, C. (1992). *Fusarium solani* cutinase is a lipolytic enzyme with a catalytic serine accessible to solvent. *Nature,* **356**, 615-618.
15. Longhi, S., Czjzek, M., Lamzin, V., Nicolas, A. & Cambillau, C. (1997). Atomic resolution (1.0 Å) crystal structure of *Fusarium solani* cutinase: stereochemical analysis. *J. Mol. Biol.* **268**, 779-799.
16. Ghosh, D., Erman, M., Sawicki, M., Lala, P., Weeks, D. R., Li, N., Pangborn, W., Thiel, D. J., Jörnvall, H., Gutierrez, R. & Eyzaguirre, J. (1999). Determination of a protein structure by iodination: the structure of iodinated acetylxylan esterase. *Acta Crystallog. sect. D,* **55**, 779-784.
17. Arpigny, J. L. & Jaeger, K.-E. (1999). Bacterial lipolytic enzymes: classification and properties. *Biochem. J.* **343**, 177-183.
18. Kabsch, W. & Sander, C. (1983). Dictionary of protein secondary structures: pattern recognition of hydrogen-bonded and geometrical features. *Biopolymers,* **22**, 2577-2637.
19. Luzzati, V. (1952). Traitement statistique des erreurs dans la détermination des structures cristallines. *Acta Crystallog.* **5**, 802-810.
20. Read, R. J. (1986). Improved Fourier coefficients for maps using phases from partial structures with errors. *Acta Crystallog. sect. A,* **42**, 140-149.
21. Jaeger, K.-E., Ransac, S., Koch, H. B., Ferrato, F. & Dijkstra, B. W. (1993). Topological characterization and modeling of the 3D structure of lipase from *Pseudomonas aeruginosa*. *FEBS Letters,* **332**, 143-149.
22. Misset, O., Gerritse, G., Jaeger, K. E., Winkler, U., Colson, C., Schanck, K., Lesuisse, E., Dartois, V., Blaauw, M., Ransac, S. & Dijkstra, B. W. (1994). The structure-function relationship of the lipases from *Pseudomonas aeruginosa* and *Bacillus subtilis*. *Protein Eng.* **7**, 523-529.
23. Jaeger, K.-E., Ransac, S., Dijkstra, B. W., Colson, C., van Heuvel, M. & Misset, O. (1994). Bacterial lipases. *FEMS Microbiol. Rev.* **15**, 29-63.
24. Uppenberg, J., Hansen, M. T., Patkar, S. & Jones, T. A. (1994). The sequence, crystal structure determination and refinement of two crystal forms of lipase B from *Candida antarctica*. *Structure,* **2**, 293-308.
25. Holm, L. & Sander, C. (1996). Mapping the protein universe. *Science,* **273**, 595-602.
26. Longhi, S., Mannesse, M., Verheij, H. M., De Haas, G. H., Egmond, M., Knoops-Mouthuy, E. & Cambillau, C. (1997). Crystal structure of cutinase covalently inhibited by a triglyceride analogue. *Protein Sci.* **6**, 275-286.
27. Lang, D. A., Mannesse, M. L. M., de Haas, G. H., Verheij, H. M. & Dijkstra, B. W. (1998). Structural basis of the chiral selectivity of *Pseudomonas cepacia* lipase. *Eur. J. Biochem.* **254**, 333-340.
28. Nardini, M., Lang, D. A., Jaeger, K.-E. & Dijkstra, B. W. (2000). Crystal structure of *Pseudomonas aeruginosa* lipase in the open conformation: the prototype for family I. 1 of bacterial lipases. *J. Biol. Chem.* **275**, 31219-31225.
29. Kim, K. K., Song, H. K., Shin, D. H., Hwang, K. Y. & Suh, S. W. (1997). The crystal structure of a triacylglycerol lipase from *Pseudomonas cepacia* reveals a highly open conformation in the absence of a bound inhibitor. *Structure,* **5**, 173-185.
30. Ransac, S., Blaauw, M., Lesuisse, E., Schanck, K., Colson, C. & Dijkstra, B. W. (1994). Crystallization and preliminary X-ray analysis of a lipase from *Bacillus subtilis*. *J. Mol. Biol.* **238**, 857-859.
31. Otwinowski, Z. & Minor, W. (1997). Processing of X-ray diffraction data collected in oscillation mode. *Methods Enzymol.* **276**, 307-326.
32. French, S. & Wilson, K. (1978). On the treatment of negative intensity observations. *Acta Crystallog. sect. A,* **34**, 517-524.
33. De la Fortelle, E. & Bricogne, G. (1997). Maximum-likelihood heavy-atom parameter refinement for multiple isomorphous replacement and multiwavelength anomalous diffraction methods. *Methods Enzymol.* **276**, 472-494.
34. Collaborative Computational Project Number 4 (1994). The CCP4 suite: programs for protein crystallography. *Acta Crystallog. sect. D,* **50**, 760-763.
35. Perrakis, A., Sixma, T. K., Wilson, K. S. & Lamzin, V. S. (1997). wARP: improvement and extension of crystallographic phases by weighted averaging of multiple-refined dummy atomic models. *Acta Crystallog. sect. D,* **53**, 448-455.
36. Van Asselt, E. J., Perrakis, A., Kalk, K. H., Lamzin, V. S. & Dijkstra, B. W. (1998). Accelerated X-ray structure elucidation of a 36 kDa muramidase/transglycosylase using wARP. *Acta Crystallog. sect. D,* **54**, 58-73.
37. Perrakis, A., Morris, R. & Lamzin, V. S. (1999). Automated protein model building combined with iterative structure refinement. *Nature Struct. Biol.* **6**, 458-463.
38. Brünger, A., Adams, P. D., Clore, G. M., Delano, W. L., Gros, P., Grosse-Kunstleve, R., Jiang, J.-S., Kuszewski, J., Nilges, M., Pannau, N. S., Read, R. J.,

Rice, L. M., Simonson, T. & Warren, G. L. (1998). Crystallography and NMR system: a new software suite for macromolecular structure determinations. *Acta Crystallog. sect. D,* **54**, 905-921.
39. Laskowski, R. A., MacArthur, M. W., Moss, D. S. & Thornton, J. M. (1993). PROCHECK: a program to check the stereochemical quality of protein structures. *J. Appl. Crystallog.* **26**, 283-291.
40. Kraulis, P. J. (1991). MOLSCRIPT: a program to produce both detailed and schematic plots of protein structures. *J. Appl. Crystallog.* **24**, 946-950.

Edited by R. Huber

(Received 5 January 2001; received in revised form 26 March 2001; accepted 26 March 2001)